NJC

Accepted Manuscript

This is an *Accepted Manuscript*, which has been through the Royal Society of Chemistry peer review process and has been accepted for publication.

Accepted Manuscripts are published online shortly after acceptance, before technical editing, formatting and proof reading. Using this free service, authors can make their results available to the community, in citable form, before we publish the edited article. We will replace this *Accepted Manuscript* with the edited and formatted *Advance Article* as soon as it is available.

You can find more information about *Accepted Manuscripts* in the Information for Authors.

Please note that technical editing may introduce minor changes to the text and/or graphics, which may alter content. The journal's standard Terms & Conditions and the Ethical guidelines still apply. In no event shall the Royal Society of Chemistry be held responsible for any errors or omissions in this *Accepted Manuscript* or any consequences arising from the use of any information it contains.

ROYAL SOCIETY OF CHEMISTRY

www.rsc.org/njc

Journal Name

ARTICLE

Hydrogen bond-assisted crystallization: structure, growth and characterization of a new mixed-anion transition metal fluoride $Na_3NH_4(TiF_6)(SO_4)\cdot H_2O$†

Received 00th January 20xx,
Accepted 00th January 20xx

DOI: 10.1039/x0xx00000x

www.rsc.org/

Dongdong Xu,[a,b] Fangfang Zhang,[a,*] Yanzhou Sun,[a] Zhihua Yang,[a] Xiaoyu Dong,[a] Shilie Pan[a,*]

The first mixed-anion transition metal (TM) fluoride with $[MF_6]^{x-}$ (M = TM cation) anion group, $Na_3NH_4(TiF_6)(SO_4)\cdot H_2O$ (NTS), was synthesized by a facile hydrothermal method. The structure of NTS features hydrogen-bonded layers constructed by four kinds of building blocks, i.e., $[NH_4]^+$, $[TiF_6]^{2-}$, $[SO_4]^{2-}$, H_2O and four categories of hydrogen bonds, i.e., N–H···O, N–H···F, O–H···O and O–H···F, and the layers are further connected by Na^+ forming a three-dimentional framework. The transparent crystal with size up to 5.0 × 2.5 × 1.0 mm^3 has been grown just by controlling the hydrothermal conditions. The crystal morphology, electronic structure, optical and thermal properties of NTS were analyzed.

Introduction

Inorganic transition metal (TM) fluorides are of topical interest owing to their significant importance in the advanced devices as the key function materials with many vital physical properties, that is, multiferroism,[1] high Tc superconductivity,[2] ferroelasticity, ionic conductivity,[3] and magnetism,[4] etc. Thus, the study on new structural types of TM fluorides is a meaningful and interesting work. As a widely accepted material design strategy, the combination of different types of anionic groups into one compound is a valuable method in solid state chemistry for the design and synthesis of new function materials. Such synthetic route is widely applied in the fields of molecular sieves (aluminophosphate,[5] aluminosilicates[6]), catalysts (polyoxometalates[7]), nonlinear optical materials (borophosphates,[8] borosilicates,[9] borocarbonates,[10] boronitrates[11]), etc. Based on these ideas, a lot of efforts were made to apply these design routes to TM fluoride system and a series of mixed-anion TM fluorides[12] were obtained successively, for instance, $KCu(CO_3)F$[13] with mixed $[CuO_2F_2]^{4-}$ and $[CO_3]^{2-}$ anions; $K_{16}[Ti_{10}(PO_4)_4F_{44}]$[14] with mixed $[TiOF_5]^{3-}$, $[TiO_2F_4]^{4-}$, $[TiO_3F_3]^{5-}$ and $[PO_4]^{3-}$ anions; Tavorite-type fluorides $LiM(SO_4)F$ (M = Co, Ni)[15] with mixed $[MO_4F_2]^{8-}$ and $[SO4]^{2-}$ anions; $Ba_2[Ti_2F_2O_2(Si_2O_7)]$[16] with mixed $[TiO_5F]^{7-}$ and $[SiO_4]^{4-}$ anions etc. These compounds feature the connection of different types of anions via bridging oxygens and can be viewed as typical mixed-anion TM fluorides.

However, when it comes to the perfluorinated group $[MF_6]^{x-}$ (M = TM cation), the implementation of such design route, that is, the synthesis of mixed-anion fluorides with $[MF_6]^{x-}$ anions, encountered unprecedented obstacles, which even becomes challenge for chemical synthesis. In the unique $[MF_6]^{x-}$ anion, bridging oxygen atoms are completely substituted by fluorine atoms due to the replaceability of oxygen and fluorine atoms in TM coordination polyhedra. Owing to the restriction of easy decomposition of $[MF_6]^{x-}$ anions with the volatilization of the F elements under high temperature, the major challenge in this area is how to limit the fluorine volatilization thus protecting $[MF_6]^{x-}$ anions from the decomposition. Although the $[MF_6]^{x-}$ anions are common in reported compounds, for example, $[VF_6]^{3-}$ anions in Na_3VF_6,[17a] $[NbF_6]^{2-}$ in Li_2NbF_6,[17b] $[CrF_6]^{3-}$ in K_3CrF_6,[17c] and $[MoF_6]^-$ in $NaMoF_6$,[17d] etc., to the best of our knowledge, mixed-anion TM fluorides containing $[MF_6]^{x-}$ anions have not been achieved up to now.

For the TM fluorides synthesis,[12] a commonly used method is the traditional two-step solid-state synthesis (first step for the composition of raw materials; second step for anionic polymerization at higher temperature),[18] however, which is often limited by the volatilization of F elements under high temperature. Other techniques have been developed, such as, traditional coprecipitation by the fast microwave heating technique for nano-particles;[19] ceramic route with a direct fluorination of the TM oxides or salts under F_2 (from the decomposition of anhydrous HF or XeF_2 etc.) atmospheres for powder samples;[20] and Czochralski method under fluorinated atmosphere for large single crystals,[21] etc. For comparison, hydrothermal method is very attractive for chemists to prevent $[MF_6]^{x-}$ anions from decomposition and avoid the volatilization of the F elements in terms of the enclosed system at low temperature without complicated devices and harsh conditions.

[a] Key Laboratory of Functional Materials and Devices for Special Environments, Xinjiang Technical Institute of Physics & Chemistry, Chinese Academy of Sciences; Xinjiang Key Laboratory of Electronic Information Materials and Devices, 40-1 South Beijing Road, Urumqi 830011, China.
[b] University of Chinese Academy of Sciences, Beijing 100049, China.
*To whom correspondence should be addressed. Emails: ffzhang@ms.xjb.ac.cn (Fangfang Zhang), slpan@ms.xjb.ac.cn (Shilie Pan).

† Electronic Supplementary Information (ESI) available: hydrothermal conditions and crystal pictures for Test 1-6，detailed crystal data, asymmetric unit, XRD, band structure and densities of states. CCDC 1451632. For ESI and crystallographic data in CIF or other electronic format.

Herein, we report the first mixed-anion TM fluoride containing anionic group $[MF_6]^{2-}$, $Na_3NH_4(TiF_6)(SO_4)\cdot H_2O$ (NTS) synthesized by a facile hydrothermal method. The transparent crystal with size up to 5.0 × 2.5 × 1.0 mm^3 has been grown and the effect of the solvent water on the product has been discussed. The crystal structure of NTS including four kinds of building blocks, i.e., $[NH_4]^+$, $[TiF_6]^{2-}$, $[SO_4]^{2-}$, H_2O and four categories of hydrogen bonds, i.e., N–H···O, N–H···F, O–H···O and O–H···F has been described. In addition, optical and thermal properties, first-principle calculations have been carried out on the title compound.

Experimental

Reagent. $(NH_4)_2TiF_6$ (Tianjin DaMao Chemical Co., Ltd., 99.0 %), Na_2SO_4 (Tianjin BoDi Chemical Co., Ltd., 99.0 %), NaF (Tianjin JiZhun Chemical Co., Ltd., 99.0 %).

Crystal growth. A mild hydrothermal experiment under subcritical conditions (T = 210 °C, autogenous pressure) was conducted to synthesis the single crystal of $Na_3NH_4(TiF_6)(SO_4)\cdot H_2O$. A mixture of 1.711 g (12 mmol) of Na_2SO_4, 0.164 g (4 mmol) of NaF, 0.783 g (4 mmol) of $(NH_4)_2TiF_6$ and 1 mL deionized water was sealed in an autoclave (23 mL) equipped with a Teflon liner. The autoclave was heated at 210 °C for 4 days and cooled to room temperature at a rate of 4 °C/h. After washed by ethanol, colourless block-shaped crystals were collected in a yield of ca. 95 % based on Ti. The powder X-ray diffraction (XRD) proved the phase purity of NTS (Figure S1 in the ESI†).

Structure determination. A single crystal of NTS in the size 0.341 × 0.165 × 0.124 mm^3 was selected for the single-crystal data collection. Data were collected on a Bruker SMART APEX II CCD diffractometer with monochromatic Mo Kα radiation (λ = 0.71073 Å) at 293(2) K and integrated with the SAINT-Plus program.[22a] The numerical absorption corrections were carried out using the SADABS program for area detector. The calculation was completed using the SHELXTL crystallographic software package.[22b] The structure was solved by the direct methods[22c] and refined by full matrix least-squares techniques with anisotropic thermal parameters. Final least-squares refinements were on F_o^2 with data having $F_o^2 \geqslant 2\sigma(F_o^2)$. All hydrogen atoms were fixed by fourier difference graph method. PLATON[22d] was used to check possible missing symmetry of the structure. Final structure refinement information and crystallographic data are listed in Tables 1 and 2. To prove the structural reasonability, the bond valence sum (BVS) calculations[23] were performed on the basis of parameters reported by Brese and O'Keeffe[23b] and results can be found in Table 2. Anisotropic displacement parameters are listed in Table S1 in the ESI†.

Fourier-transform Infrared (FT-IR) spectroscopy. For the verification of the existence of $[TiF_6]^{2-}$ and $[SO_4]^{2-}$ anions, FT-IR spectroscopy (KBr pellet) was conducted on a Shimadzu IR Affinity-1 FT-IR spectrometer with a resolution of 1 cm^{-1}. The data were collected for the scope of 4000 - 400 cm^{-1} in air.

Table 1. Crystal data and structure refinement information.

formula	$Na_3NH_4(TiF_6)(SO_4)\cdot H_2O$
Formula weight /g·mol^{-1}	362.99
Crystal system	Orthorhombic
Space group, Z	*Pnma*, 4
a/ Å	12.925(13)
b/Å	7.971(8)
c/Å	9.546(10)
Density/ g·cm^{-3}	2.452
Absorption coefficient (mm^{-1})	1.316
F(000)	712
θ_{max}/deg.	27.47
Limiting indices	$-16 \leq h \leq 15$, $-10 \leq k \leq 5$, $-12 \leq l \leq 11$
Reflections collected / unique	5716/1208 [R(int) = 0.0368]
Completeness	99.8%
Data/restraints/parameters	1208 / 0 / 105
GOF on F^2	1.078
Final R indices [$F_o^2 > 2\sigma(F_o^2)$][a]	R_1 = 0.0315, wR_2 = 0.0798
R indices (all data)[a]	R_1 = 0.0390, wR_2 = 0.0843
Extinction coefficient	0.0053(13)
Largest diff. peak and hole (e·Å^{-3})	0.493 and – 0.542

[a] $R_1 = \Sigma||F_o| - |F_c|| / \Sigma|F_o|$ and $wR_2 = [\Sigma w(F_o^2 - F_c^2)^2 / \Sigma wF_o^4]^{1/2}$ for $F_o^2 > 2\sigma(F_o^2)$.

Table 2. Atomic coordinates (×10^4), equivalent isotropic displacement parameters (Å^2 × 10^3), and bond valence sums.

Atoms	x	y	z	U(eq)[b]	BVS
Ti(1)	980(1)	7500	3253(1)	14(1)	4.64
Na(1)	2959(1)	9579(1)	1373(1)	32(1)	1.00
Na(2)	0	10000	0	21(1)	1.23
S(1)	1897(1)	7500	– 1542(1)	14(1)	6.08
F(1)	925(1)	9179(2)	1926(2)	27(1)	1.05
F(2)	1095(1)	9119(2)	4643(2)	26(1)	0.95
F(3)	– 443(2)	7500	3434(2)	30(1)	0.93
F(4)	2422(1)	7500	2986(2)	22(1)	1.03
O(1)	1253(2)	9008(2)	– 1607(2)	25(1)	1.93
O(2)	2583(2)	7500	– 2786(2)	23(1)	1.72
O(3)	2529(2)	7500	– 268(2)	25(1)	1.99
$O(4)_{water}$	1010(2)	12500	16(3)	25(1)	—
$N(5)_{ammonium}$	4597(3)	7500	8413(4)	26(1)	—

[b] U(eq) is defined as one third of the trace of the orthogonalized U_{ij} tensor.

UV–Vis–NIR diffuse–reflectance spectroscopy. UV-Vis-NIR diffuse–reflectance spectroscopy was measured on a Shimadzu SolidSpec-3700DUV spectrophotometer in air. The measurement range is from 200 to 2600 nm. Absorption (K/S) data are calculated based on the following Kubelka-Munk function,[24]

$$F(R) = \frac{(1-R)^2}{2R} = \frac{K}{S}$$

where R is the reflectance, K is the absorption, and S is the scattering. The band gap was deduced by the intersection point between the energy axis and the line extrapolated from the linear portion of the absorption edge.[24c]

Transmission Spectrum. The transmission spectrum of a transparent NTS crystal plate (1 mm thick, without further treatment) was recorded by Lamda 900UV/VIS/NIR (Perkin-Elmer) spectrophotometer in air. The measurement range is from 200 to 1400 nm.

Thermal analysis. The thermal behaviour of NTS was investigated with thermogravimetry (TG) and differential scanning calorimeter (DSC) using a NETZSCH STA 449F3

simultaneous thermal analyser. The sample was heated under flowing N_2 at a rate of 10 °C/min from 40 to 1200 °C.

First-principle calculations. Single crystal structural data of NTS were used for the theoretical calculations. Band structures and density of states were performed using the density functional theory method based the ab initio implemented in the CASTEP package.[25a] During the calculation, we adopted the perdew-burke-ernzerh (PBE) of functional within the generalized gradient approximation (GGA) scheme as the exchange-correlation potential.[25b] Under the norm-conserving pseudopotential, pseudo atomic calculation performed for atoms are: H, $1s^1$; N, $2s^22p^3$; O, $2s^22p^4$; F, $2s^22p^5$; Na, $2s^22p^63s^1$; S, $3s^23p^4$; Ti, $3s^23p^63d^24s^2$. The plane-wave energy cutoff was set at 940 eV, and the numerical integration of the Brillouin zone was investigated using a 3 × 4 × 3 Monkhorst-Pack *k*-point sampling.

Results and discussion

Crystal growth. For the larger and higher quality single crystals, a series of tests were performed at the same temperature by adjusting the hydrothermal conditions. The hydrothermal conditions and the representative crystal pictures for Tests 1 - 6 are listed in Table S2 and Figure S2 respectively in the ESI†. In all tests, NTS crystals were obtained in yields larger than 90 % based on Ti, however, the crystal sizes or quality were different. In Tests 1-4, 23 mL autoclaves were employed. Crystals with the average size of 6.0 × 5.0 × 4.0 mm^3 were obtained in Test 1, but containing lots of defects. In order to increase the crystal quality, the volume of solvent water was increase to 2, 3, 4 mL in Tests 2 - 4, respectively, with respect to 1 mL in Test 1. It was found that with the increase of the filling degree in the Tests 1 - 4, NTS crystals become more transparent while crystal sizes decrease. As a result, the single crystal with the size of 5.0 × 2.5 × 1.0 mm^3 was grown in the optimal condition of Test 2, which possess the balance between size and quality (see Figure 1c). One possible reason for the phenomenon could be explained based on the following understanding. More solvent water means larger dissolving capacity and lower concentration of reagents. Firstly, lower concentration is beneficial to diffusion process of growth units from solution to growth interface and suppress the defect generation. Secondly, the larger dissolving capacity results in more regents in water after the completion of crystallization, which leads to less growth units for the crystal growth. The above two points maybe explain the reason why NTS crystals grow better with smaller size as the volume of water increasing.

In Tests 5 and 6, 100 ml autoclaves were used and the quantities of reactants as well as the solvent were increased by 3 and 10 times compared with Test 1, respectively. NTS crystals with uniform morphology and size (average size, ca. 6.0 × 3.0 × 2.0 mm^3) were obtained. The crystal morphology is a reflection of its structure. Based on Bravais-Friedel and Donnay-Harker (BFDH) methods,[26a] the theoretical morphology of NTS (Figure 1a) was simulated using mercury program.[26b] We can see that the as-grown NTS crystal prepared

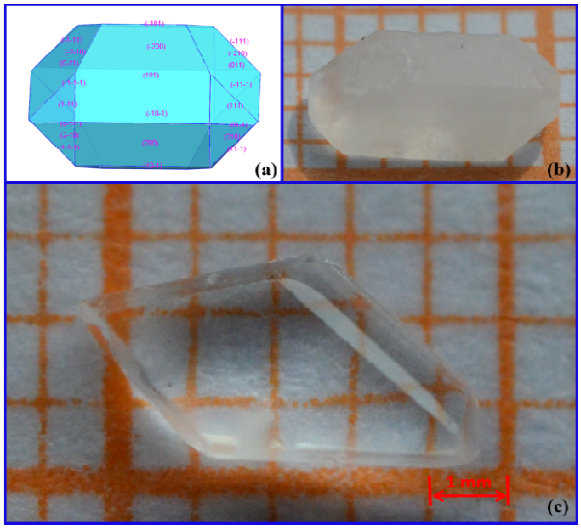

Figure 1. (a) Theoretical morphology of NTS. (b) The as-grown NTS crystal in Test 5. (c) Photograph of single crystal for NTS.

in Test 5 (Figure 1b) is consistent with the ideal morphology. Experimentally, the NTS crystal is still transparent after exposed in air at room temperature for two weeks. The test for the solubility shows that the crystal is easily soluble in water.

In most cases, solid state mixed-anion fluorides of TMs reported previously are nano-particles, powders or microcrystals.[27] Here, single crystals of NTS with size up to 5.0 × 2.5 × 1.0 mm^3 (Figure 1c) were grown indicating the effectivity of the mild hydrothermal method. It is expected that other mixed-anion fluorides with $[MF_6]^{x-}$ anions could also be obtained via the hydrothermal method introduced in this paper with proper $[MF_6]^{x-}$ anion-based precursors and reaction conditions.

Structure description. According to single-crystal XRD analysis, NTS crystallizes in the orthorhombic crystal system with the space group *Pnma* (no. 62). In the asymmetric unit (Figure S3 in the ESI†), there are one crystallographically distinct Ti site (4c), one S site (4c), one N site (4c), two Na sites (8d, 4a), four O sites (8d, 8d, 4c, 4c) and four F sites (8d, 4c, 4c, 4c). The central Ti(1) atom is six-coordinated by six fluorine atoms to form the $[TiF_6]^{2-}$ octahedra with Ti-F bond distances in the range of 1.844(19) - 1.881(3) Å (av. 1.855 Å) and F-Ti-F angles in the range of 86.84(7) - 93.06(12) ° (av. 90.00 °). The S(1) atom adopts tetrahedral coordination, forming the $[SO_4]^{2-}$ tetrahedra in which the S-O bond distances varies from 1.464(2) to 1.482(3) Å (av. 1.468Å) and O-S-O angles vary from 107.83(9) to 110.66(9)° (av. 109.45°). In addition, N(1) and O(4) exist in the form of $[NH_4]^+$ and crystalline water, respectively. Selected bonds are listed Table S3 in the ESI†. These data mentioned above agree with compounds containing $[TiF_6]^{2-}$ or $[SO_4]^{2-}$ previously reported.[28]

The results of BVS calculations give reasonable values for all the atoms except that the value is too large for Ti^{4+} (4.64

v.u.). The similar conditions can be found in structures reported in the earlier literatures, for example, K_2TiF_6 (4.57 v.u.),[28a] $(NH_4)_2TiF_6$ (4.52 v.u.),[29a] $Li(NH_4)TiF_6$ (4.69 v.u.),[29b] $AgTiF_6$ (4.34 v.u.),[29c] $BaTiF_6$ (4.71 v.u.),[29d] $K_2(HF)TiF_6$ (4.58 v.u.).[29e] Thus, considering other characterization methods in this paper, we can conclude that the structure is correct in spite of the large deviation. One possible cause could be the overestimate for bond valence of Ti-F bond especially for shorter ones (< 1.9 Å).

Figure 2 shows the structure of NTS. In the structure, the $[TiF_6]^{2-}$ octahedra and $[SO_4]^{2-}$ tetrahedra are separated by $[NH_4]^+$ and H_2O, and these four kinds of building blocks distribute in the same ac-plane periodically to form a layer. Then these layers are stacked up along the b axis to construct the whole structure with the Na-O and Na-F bonds connecting the adjacent layers. To the best of our knowledge, NTS is the first mixed-anion TM fluoride containing $[MF_6]^{x-}$ anions. Furthermore, unlike typical type of mixed-anion TM fluorides whose different types of anions were connected via bridging oxygen atoms to form 0D large limited polyanions,[14] 1D infinite chains,[27b] 2D layers,[30] or a 3D network,[16] NTS features isolated $[TiF_6]^{2-}$ and $[SO_4]^{2-}$ anions, which can be described as a new type of mixed-anion TM fluorides.

When analysing the details of the structure, interestingly, we found that the structure features enormous amount of hydrogen bonds in the ac-plane which can be classified into four categories, i.e., N–H···O, N–H···F, O–H···O and O–H···F bonds (Figure 3). The length and angles of hydrogen bonds can be found in Table S4 in the ESI†. In layers, these hydrogen bonds play a significant role in the connection of $[TiF_6]^{2-}$ and $[SO_4]^{2-}$ anions, and increase the structural stability. Actually,weak intermolecular interactions are often regarded as an important role when constructing structures. Many strategies for crystal engineering include the use of various intermolecular forces, mostly, hydrogen bonding.[31] For example, in supramolecular self-assembly field, large organic molecules or groups play the role of hydrogen bond donors and acceptors. While in the layers of NTS, different from supramolecular, small inorganic units $[NH_4]^+$ and H_2O act as good hydrogen bond donors and $[TiF_6]^{2-}$ and $[SO_4]^{2-}$ anions are good hydrogen bond acceptors. This interesting finding opens new perspective

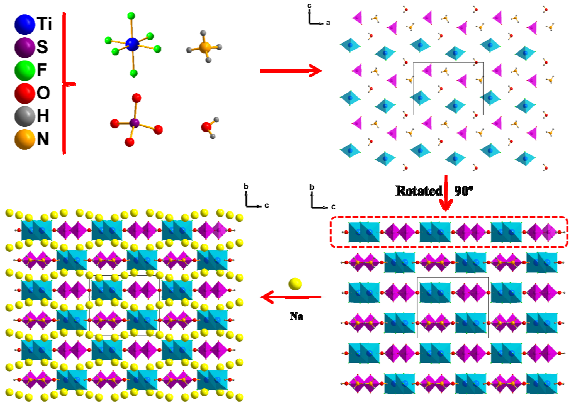

Figure 2. Polyhedral view of the structure.

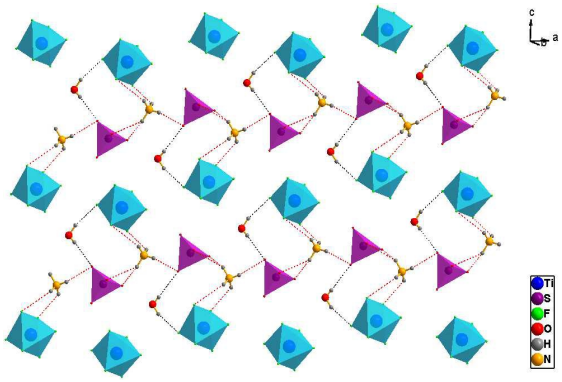

Figure 3. The assembly of four building blocks via four categories of hydrogen bonds, i.e., N–H···O, N–H···F, O–H···O and O–H···F, which contribute to the stability in layers.

in the design and synthesis of such inorganic small-molecular fluorides. Except traditional covalent bonded framework and strong Coulombic forces between cations and anions, cooperative hydrogen-bonded coordination network could take subsidiary function for the linkage of anions in inorganic structure.

Figure 4 shows a 3D framework constructed by Na-O/F ionic bonds. It exhibits eight-membered rings built by two types of Na-based chains, named $[Na(1)O_2F_3]_\infty$ and $[Na(2)O_2F_2(H_2O)]_\infty$, respectively. Specifically, the $Na(1)O_3F_4$ units are connected by the O(2), O(3), F(3), F(4) atoms to form the $[Na(1)O_2F_3]_\infty$ chains. Zigzag chains $[Na(2)O_2F_2(H_2O)]_\infty$ are composed of the $Na(2)O_2F_2(H_2O)_2$ octahedra with crystalline water H_2O bridging the adjacent octahedra. This 3D framework provides a strong Coulombic field which plays a decisive role in the construction of the crystal. It can be concluded that the stability of NTS is determined by strong Coulombic field built by four cations and two dianions, and a large amount of hydrogen bonding reciprocity take subsidiary function for the structure.

Optical properties. FT-IR spectrum for NTS is shown in Figure 5a. The characteristic absorption peaks of samples were assigned to their corresponding functional groups as follows[32]:

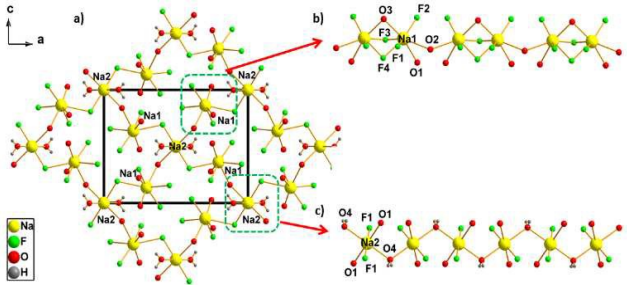

Figure 4. (a) 3D network built by Na-F and Na-O ionic bonds that play an important role for the stability between layers. (b) Na(1) chains: $[Na(1)O_2F_3]_\infty$ constructed by the $Na(1)O_3F_4$ units.

(c) Na(2) chains: $[Na(2)O_2F_2(H_2O)]_\infty$ composed of $Na(2)O_2F_2(H_2O)_2$ octahedra.

of the conduction bands and the top of the valence bands lie in the G point indicating that it is a direct bandgap compound. The

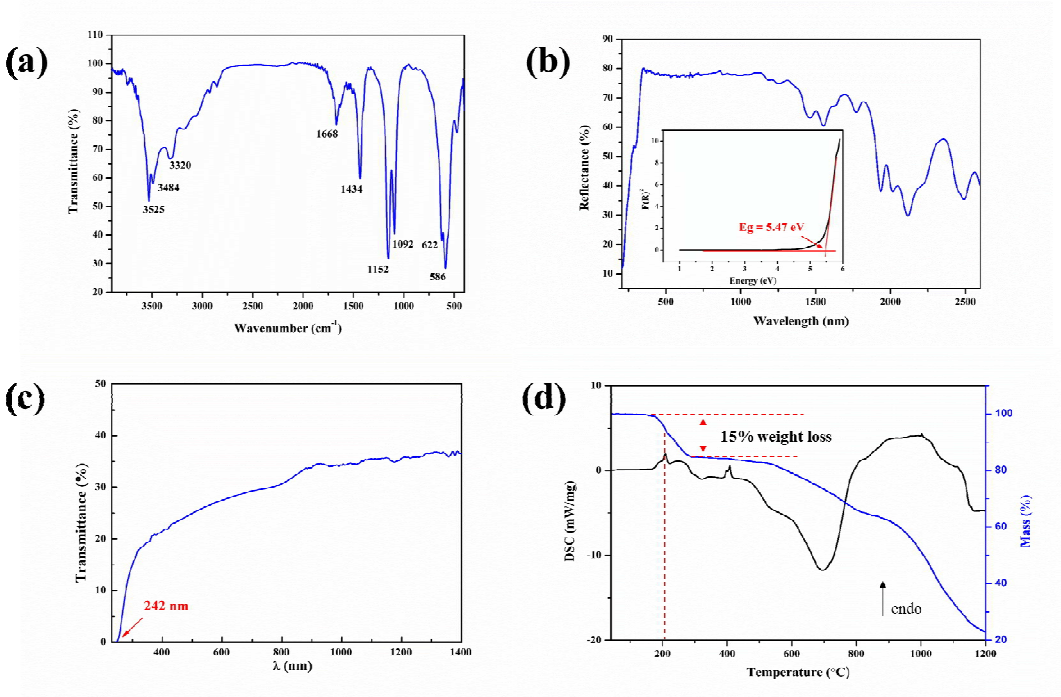

Figure 5. Thermal properties and optical properties of NTS: (a) FT-IR spectroscopy; (b) UV–Vis–NIR diffuse–reflectance spectroscopy. Insert: plot of transformed Kubelka-Munk function versus the energy of the light adsorbed; (c) Transmission spectrum; (d) TG-DSC curves.

the strong absorption peaks at 586, 622 cm^{-1} can be assigned to the stretching vibrations ν(Ti-F) and in-plane degenerate bending vibrations δ_d(O-S-O); the strong absorption peaks at 1092, 1152 cm^{-1} are likely degenerate stretching vibrations ν_d(S-O); the medium absorption peak at 1434 cm^{-1} is related to in-plane degenerate bending vibrations δ_d(H-N-H); the weak absorption peak at 1668 cm^{-1} is assigned to degenerate stretching vibrations ν_d(H-O-H); stretching vibrations ν(O-H) and degenerate stretching vibrations ν_d(N-H) displays strong absorption bands in the range of 2700 - 3600 cm^{-1}. The IR spectrum confirms the existence of $[TiF_6]^{2-}$, $[SO_4]^{2-}$, H_2O and $[NH_4]^+$ units. The optical diffuse reflectance spectrum (Figure 5b) indicates the band gap is 5.47 eV, which is consistent with cut-off edge derived from transmission spectrum (Figure 5c).

Thermal behaviour. TG-DSC curves show a continuous decomposition process of NTS as the temperature increasing (Figure 5d). At about 200 °C, an obvious weight loss can be observed on the TG curve and a clear endothermic peak on the DSC curve. The observed weight loss of 15 % well matches with the release of 1 mol of HF, 1 mol of NH_3 and 1 mol of H_2O per 1 mol of NTS molecules whose calculated value is 15.16 %, which could help understanding the possible decomposition mechanism.

Band structure and density of states. The band structure of NTS is shown in Figure S4a in the ESI†. It is found that the bottom GGA-PEB band gap is 3.20 eV, which is smaller than experimental value obtained by the transmission spectrum. It is well known that GGA always underestimate the bandgap due to the insufficient accuracy of exchange correlation energy.[33] The projected densities of states diagrams are shown in Figure S4b in the ESI†. In the range of – 6 ~ – 1 eV, strong bonding in $[TiF_6]^{2-}$ anions makes a wide separation between T-d states and F-p states. The overlap between O-s states and S-p states implies a covalent bond character of S-O bond. In the vicinity to Fermi level, there are O-p states, H-s states, Na-p states. It clearly shows that the dominant component is O-2p orbitals from $[SO_4]^{2-}$ anion groups. For the range of 3 ~ 6 eV, Ti-d states are the dominant component. To summarize, the bottom of conduction bands and top of valence bands are occupied by the anti-bond orbitals of Ti-F and O-2p orbitals, respectively, which implies that the interaction between titanium and fluorine narrows the bandgap.

Conclusions

A facile hydrothermal method has been successfully used to synthesize single crystal of NTS, the first mixed-anion TM fluoride with isolated $[TiF_6]^{2-}$ and $[SO_4]^{2-}$ anions. The stability of NTS is determined by strong Coulombic field built by four

cations and two dianions, which sheds some light on why these $[TiF_6]^{2-}$ and $[SO_4]^{2-}$ anions can coexist in one compound steadily. A large amount of hydrogen bonding reciprocity takes subsidiary function for the crystallization. It is worth mentioning that, likely the future hydrogen bond donors and acceptors, e.g. small-inorganic groups $[NH_4]^+$, H_2O, $[TiF_6]^{2-}$ and $[SO_4]^{2-}$ etc. have to be taken into account for designing new inorganic compounds and for modulating their properties.

Acknowledgements

The authors acknowledge the financial support by Xinjiang Key Laboratory Foundation (Grant No. 2014KL009), National Natural Science Foundation of China (Grant Nos. 21301189, U1503193, 51425206, 2014CB648400), the Xinjiang International Science & Technology Cooperation Program (20146001), and the Science and Technology Project of Urumqi (Grant P141010005), the Foundation of the Youth Innovation Promotion Association of CAS.

References

1 (a) J. F. Scott and R. J. Blinc, *Phys.: Condens. Matter.*, 2011, **23**, 113202; (b) J. J. Ravez, *Phys.*, 1997, **III7**, 1129.
2 (a) J. B. Bednorz and K. A. Z. Muller, *Phys. B.*, 1986, **64**, 189; (b) B. Chevalier, A. Tressaud, B. Lepine, K. Amine, J. M. Dance, L. Lozano,E. Hickey andJ. Etourneau,*Physica. C.*, 1990, **167**, 97.
3 A. K. Ivanov-Shits, N. I. Sorokin, P. P. Fedorov andB. P. Sobolev,*Solid. State. Ionics.*, 1989, **31**, 253.
4 (a) M. D. Donakowski, A. Go¨rne, J. T. Vaughey, and K. R. Poeppelmeier, *J. Am. Chem. Soc.*, 2013, **135**, 9898; (b) S. W. Kim, H. Y. Chang and P. S. Halasyamani, *J. Am. Chem. Soc.*, 2010, **132**, 17684;(c)J. M. Dance, A. Tressaud, Ferro- and Ferrimagnetism inFluorides. In *Inorganic Solid Fluorides*; P. Hagenmuller, Ed.; AcademicPress: New York, 1985; Chapter **9**, 371;
5 (a) J. H. Yu and R. R. Xu, *Acc. Chem. Res.*, 2003, **36**, 481; (b) M. E. Davis, C. Saldarriage and C. Montes, *Nature*, 1988, **331**, 698; (c) A. K. Cheetham, G. Ferey and T. Loiseau, *Angew. Chem. Int. Ed.*, 1999, **38**, 3268.
6 M. E. Davis, *Nature*, 2002, **417**, 813.
7 (a) S. S. Wang and G. Y. Yang, *Chem. Rev.*, 2015, **115**, 4893; (b) J. F. Keggin, *Nature*, 1933, **131**, 908; (c) J. S. Anderson, Nature, 1937, **140**, 850.
8 (a) R. Kniep, G. Gpezel, B. Eisenmann, C. Roehr, M. Asbrand and M. Kizilyalli, *Angew. Chem.*, 1994, **106**, 791; (b) S. L. Pan, Y. C. Wu, P. Z. Fu, G. C. Zhang, Z. H. Li, C. X. Du and C. T. Chen, *Chem. Mater.*, 2003, **15**, 2218; (c) Y. Wang, S. L. Pan, Y. J. Shi, *Chem. Eur. J.*, 2012, **18**, 12046.
9 (a) H. P. Wu, H. W. Yu, S. L. Pan, Z. J. Huang, Z. H. Yang, X. Su and K. R. Poeppelmeier, *Angew. Chem. Int. Ed.*, 2013, **52**, 3406; (b) M. G.Krzhizhanovskayal, R. S. Bubnova, and S. K. *Filatovl, J. Struct. Chem.*, 2014, **55**, 1342.
10 M. Abudoureheman, L. Wang, X. M. Zhang, H. W. Yu, Z. H. Yang, C. Lei, J. Han and S. L. Pan, *Inorg. Chem.*, 2015, **54**, 4138.
11 (a) F. Kong, C. L. Hu, M. L. Liang and J. G. Mao, *Inorg. Chem.,* 2016, **55**, 948; (b) J. L. Song, C. L. Hu, X. Xu, F. Kong and J. G. Mao, *Angew. Chem. Int. Ed.*, 2015, **127**, 3750; (c) B. C. Zhao, W. Sun, W. J. Ren, Y. X. Huang, Z. C. Li, Y. M. Pan and J. X. Mi, *J. Solid State. Chem.,* 2013, **206**, 91.
12 M. Leblanc, V. Maisonneuve and A. Tressaud, *Chem. Rev.*, 2015, **115**, 1191.
13 N. Mercier and M. Ie Blanc, *Chem. Eur. J.*, 1994, **31**, 423.
14 S. H. Yang, G. B. Li, A. J. Blake, J. L. Sun, M. Xiong, F. H. Liao and J. H. Lin, *Inorg. Chem.*, 2008, **47**, 1414.
15 P. Barpanda, N. Recham, J. N. Chotard, K. Djellab, W. Walker, M. Armandaand J. M. Tarascon, *J. Mater. Chem.*, 2010, **20**, 1659.
16 M. Mann and J. Kolis, *ActaCrystallogr., Sect. C: Cryst. Struct. Commun.*, 2009, **65**, 17.
17 (a) E. Alter and R. Hoppe, *Z. Anorg. Allg. Chem.,* 1975, **412**, 110; (b) O. Graudejus, A. P. Wilkinson, L. C. Chaco´n and N. Bartlett, *Inorg. Chem.*, 2000, **39**, 2794; (c) V. H. Bode and E. Voss, *Z. Anorg. Allg. Chem.,* 1957, **290**, 1; (d) A. J. Edwards and R. D. Peacock, *J. Chem. Soc.,* 1961, **1961**, 4253.
18 Y. H. Ben, M. Shikano, H. Kobayashi, M. Avdeev, S. Liu and C. D. Ling, *Dalton Trans.*, 2012, **41**, 5838.
19 P. P. Fedorov, M. N. Mayakova, S. V. V. Kuznetsov, V. Voronov, V. V. Osiko, R. P. Ermakov, I. V. Gontar, A. A. Timofeev and L. D. Iskhakova, *Nanotechnology*, 2011, **6**, 203.
20 E. Banks, Fluorine Chemistry at the Millennium: Fascinated by Fluorine, Elsevier: Amsterdam, 2000.
21 K. Shimamura, H. Sato, A. Bensalah, V. Sudesh, H. Machida, N. Sarukura and T. Fukuda, *Cryst. Res. Technol.,* 2001, **36**, 801.
22 (a) SAINT–Plus, version 6.02A Bruker Analytical X–rayInstruments, Inc.: Madison, WI, 2000; (b) G. M. Sheldrick, SHELXTL, Version 6.14 Bruker Analytical X–ray Instruments, Inc.: Madison, WI, 2003; (c) G. M. Sheldrick, SHELXS–97, Program for X–ray Crystal Structure Solution; University of Göttingen: Göttingen, Germany, 1997; (d) A. L. Spek, *J. Appl. Crystallogr.,* 2003, **36**, 7.
23 (a) I. D. Brown and D. Altermatt, *Acta Crystallogr.*, 1985, **B41**, 244; (b) N. E. Brese and M. O'Keeffe, *Acta Crystallogr.,* 1991, **B47**, 192.
24 (a) P. Kubelka and F. Munk, *Z. Tech. Phys.,* 1931, **12**, 593; (b) J. Tauc, *Mater. Res. Bull.*, 1970, **5**, 721; (c) T. J. McCarthy, S. P. Ngeyi, J. H. Liao, D. C. Degroot, T. Hogan, C. R. Kannewurf and M. G. Kanatzidis, *Chem. Mater.*, 1993, **5**, 331.
25 (a) S. J. Clark, M. D. Segall, C. J. Pickard, P. J. Hasnip,M. J. Probert, K. Rrfson and M. C. Payne, *Z. Kristallogr.,* 2005, **220**, 568; (b) D. M. Ceperley and B. J. Alder, *Phys. Rev. Lett.,* 1980, **45**, 566.
26 (a) P. Hartman, W. G. Perdok, *Am. Mineral.,* 1937, **22**, 463; (b) C. F. Macrae, I. J. Bruno, J. A. Chisholm, P. R. Edgington, P. McCabe, E. Pidcock, L. Rodriguez-Monge, R. Taylor, J. Streek and P. A. Wood, *J. Appl. Crystallogr.,* 2008, **41**, 466.
27 (a) S. H. Yang, G. B. Li, L. P. You, J. L. Tao, C. K. Loong, S. J. Tian, F. H. Liao and J. H. Lin, *Chem. Mater.,* 2007, **19**, 942; (b) S. H. Yang, G. B. Li, L. Li, S. J. Tian, F. H. Liao, M. Xiong and J. H. Lin, *Inorg. Chem.,* 2007, **46**, 11431.
28 (a) O. Goebel, *Acta Crystallogr., Sect. C: Cryst. Struct. Commun.* 2000, **56**, 521; (b) S. Arzt and A. M. Glazer, *Acta Crystallogr. Sect. B: Struct. Sci.,* 1994, **50**, 425.
29 (a) Z. Tun and I. D. Brown, *Acta Crystallogr.,* 1982, **B38**, 1792; (b) A.V. Gerasimenko, V. Y. Kavun, T. F. Antokhina and V. I. Sergienko, *Zh. Obshch. Khim.,* 1995, **40**, 1463; (c) R. Fischer and B. G. Mueller, *Z. Anorg. Allg. Chem.,* 2001, **627**, 445; (d) S. Becher, G. benner and R. Hoppe, *Z. Anorg. Allg. Chem.,* 1990, **591**, 7; (e) D. V. Peryshkov, R. Friedemann, E. Goreshnik, Z. Mazej, K. Seppelt and S. H. Strauss, *J. Fluorine Chem.,* 2013, **145**, 118.
30 K. L. Marshell and M. T. Weller, *Z. Anorg. Allg. Chem.,* 2014, **640**, 2766.
31 (a) A. N. Sokolov and L. R. MacGillivray, *Cryst. Growth Des.,* 2006, **6**, 2615; (b) W. E. Leong and J. J. Vittallii, *Cryst. Growth Des.,* 2007, **7**, 2112; (c) A. Peuronen, E. Lehtimäki and M. Lahtinen, *Cryst. Growth Des.,* 2013, **13**, 4615.

32 K. Nakamoto, Infrared and Raman Spectra of Inorganic and Coordination Compounds Part A: Theory and Applications in Inorganic Chemistry. Sixth Edition, Wiley: New Jersey, 2009.
33 (a) M.K. Chan and G. Ceder, *Phys. Rev. Lett.*, 2010, **105**, 196403; (b) J. Tauc, *Mater. Res. Bull.,* 1970, **5,** 721.

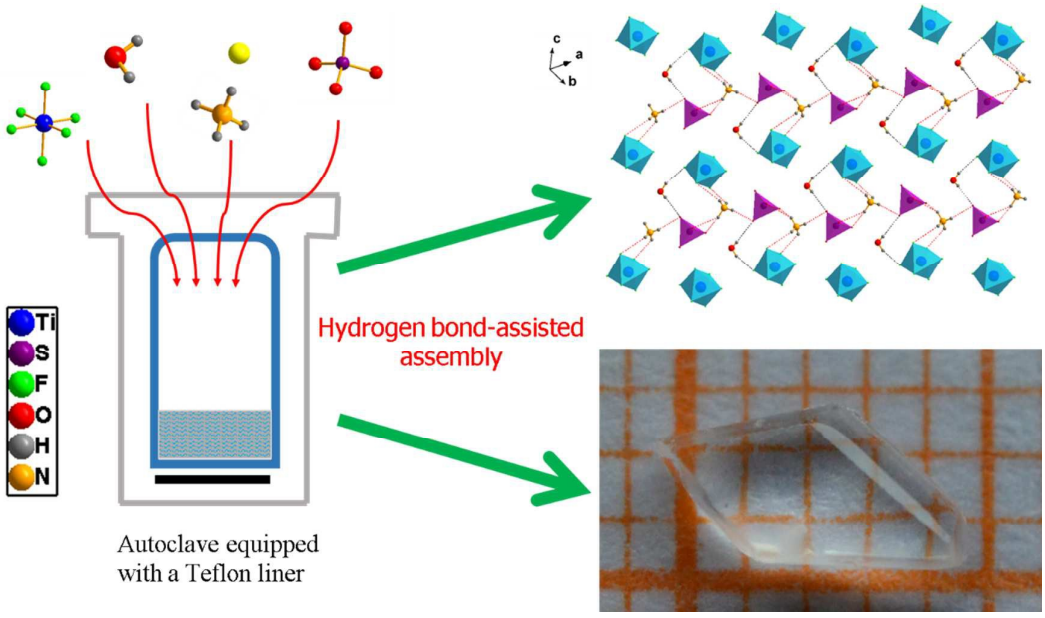

A new type of mixed-anion TM fluorides was grown with the size up to 5.0 × 2.5 × 1.0 mm^3 by a facile hydrothermal method.